A multiphase computational study of oil distribution inside roller bearings with under-race lubrication

Wenjun Gao, Kun Li, Zhenxia Liu, Yaguo Lyu, Daniel Nelias

A Multiphase Computational Study of Oil Distribution Inside Roller Bearings with Under-Race Lubrication

Wenjun GAO[a,b,*], Daniel NELIAS[b], Kun LI[a], Zhenxia LIU[a], Yaguo LYU[a]

[a] *School of Power and Energy, Northwestern Polytechnical University, Xi'an, China*
[b] *Univ Lyon, INSA-Lyon, CNRS, UMR5259 LaMCoS, F-69621, France*

Abstract

Oil-phase distribution inside roller bearings with under-race lubrication is a key element for bearing lubricating and cooling, and it determines the bearing's hydraulic loss, which may represent up to 50% of total power dissipated. The CLSVOF method for multiphase flow is conducted to track oil/air two-phase flow inside roller bearing with under-race lubrication, and quantify the influence of various factors, particularly rotating speeds of bearing components. The result demonstrates that there is an optimal oil inlet velocity to keep more oil accumulation inside bearing cavity. Exceptionally, it's found that the relative rotating between inner ring and cage could change oil volume fraction with a convex trend. While rotating speed of inner ring and outer ring changes oil volume fraction linearly.

Keywords: roller bearing; under-race lubrication; two-phase flow; oil volume fraction

1. Introduction

High speed roller bearing is commonly used as an important component in aircraft turbine engine, which needs lubricant oil to ensure its steady running and capability. Sufficient oil flow rate into the bearing is essential with an increasingly severe operating environment, to achieve sufficient lubricating

*Corresponding author
Email address: gaowenjun@nwpu.edu.cn (Wenjun GAO)

and desired temperature [1]. Larger amounts of oil flow can definitely enhance heat dissipation. However, it leads to larger capacity pump and higher power consumption of the engine. Further, larger oil feeding may increase excessive parasitic losses when rolling elements translate and rotate into the fluid environment [2], which may reach up to 50% of the total one for high speed applications (DN $> 3 \times 10^6$, bore diameter (mm) $\times$ rotating speed (rpm)). These put increasing demands on deep understanding of oil behavior inside bearing cavity, to optimize its lubricating and cooling method design.

In view that motion of moving parts of bearing will tend to induce an oil/air mixture within the bearing, it becomes necessary to quantify the oil/air volume ratio when comparing the mixture to an one-phase fluid [3]. The equivalent fluid properties are taken as those in roller drag and churning effect calculation [4]. Since heat generation and bearing temperatures are dependent on oil volume fraction inside bearing cavity[5], a detailed investigation on the oil/air two-phase flow is important and valuable.

For roller bearings, the oil/air two-phase flow in bearing chamber has been investigated a lot experimentally and numerically [6]. The works mainly focus on oil film formation, droplet adhesion, and thermal convection. Peduto et al. [7] calculated the lubricating oil movement on bearing chamber and oil return pipe wall. Flouros et al. [8] established oil film motion calculation models taking into account of oil drop/oil film interaction, evaporation of high temperature lubricating oil, air shearing and heat transfer of air/oil film/wall. Simmons et al. [9] conducted the CFD modelling method to calculate oil-gas two-phase flow and droplet trajectories in bearing chamber, and found that the flow inside bearing chamber is highly affected by the shaft, chamber structure, and the sealing air, etc.

The flow inside bearing cavity is relatively complex with intense interaction between the fluid and rolling elements [10]. Liebrecht et al. [11] investigated the influence of lubricant displacement on the total friction torque of a bearing with a vertical rotating axis. Wei et al. contribute a lot for air-oil distribution inside ball bearing with jet lubrication [12, 13]. The stratigied air-oil flow in-

side jet cooling ball bearings were studied numerically and experimentally [14]. Two experimental apparatuses were built for flow pattern and temperature distribution tests [15], to validate the numerical results. Then the uniform of oil distribution inside ball bearings was analyzed considering different parametric effects. Akinola et al. [16] presented a transient simulation of oil/air two-phase flow in bearing cavity using a coupled level-set VOF (CLSVOF) approach. It is found that the oil volume fraction is directly proportional to the shaft speed.

To sum up, the fluid flow inside high speed roller bearings with under-race lubrication is relatively unknown, with somewhat scant attention. In this article, a numerical method is employed to investigate oil/air two-phase flow behavior inside roller bearings with under-race lubrication. A detailed discussion of oil distribution along bearing circumference is proposed with different lubricating schemes and operating conditions. Particularly bearing component rotating speeds are studied separately to verify their effects.

2. Problem definition and computation domain

For under-race lubrication, lubricant oil is supplied into bearing cavity through inner race apertures by centrifugal force and high pressure. The aperture, or named the nozzle in this article, is aimed vertically at inner raceway surface and rotates along with the inner ring. Previous studies show that oil volume fraction inside bearing cavity is a function of bearing speed, oil property, and oil volume flow rate [17]. In addition, in some cases like intershaft supporting, outer ring of the bearing rotates together with inner ring, which may also exerts an impact on the oil distribution. After lubricating and cooling the bearing, the oil removes into bearing chambers on both sides of the bearing.

To simulate oil/air two-phase flow inside roller bearing with under-race lubrication, a simplified configuration is built, with 16 cylindrical cylinders as rollers, two hollow rings as inner and outer rings, and the cage. One nozzle is set to replace the aperture through the inner race for oil supplying. A schematic diagram of the cylindrical roller bearing with under-race lubrication is shown

Table 1: Roller bearing specifications with under-race lubrication

Pitch diameter(mm)	48.5
Bearing width (mm)	14
Number of rollers	16
Roller diameter(mm)	7.14
Roller length(mm)	10

in Fig. 1. The fluid domain contains the flow field inside bearing cavity and oil-inlet nozzle, hollowing all rollers and the cage between the inner and outer runways. To deal with the contact feature between rollers and raceway in practical conditions [18], there is a gap of 1/20 of roller radius between rollers and two rings in the simulation configuration. This gap is empirical but enough for the improvement of mesh quality.

In the numerical investigation, bearing chambers on both sides of the bearing is ignored and the bearing geometrical edge is taken as the flow field boundary, which is however unreasonable [19]. The oil/air flow inside bearing cavity is undoubtedly affected by bearing chambers on both sides, which play a role of boundary condition. Nevertheless, the flow inside bearing chamber is too complicated to be simulated together, with complicated oil droplet/oil film/wall/scavenge system/sealing air mixing interaction [20, 21, 22]. Thus here the flow space inside the bearing is assumed to be directly open to ambient air.

3. Numerical approach

3.1. Meshes and boundary conditions

The cylindrical roller bearing specification used in the numerical investigation is listed in Table 1. The flow field inside the bearing is discretized with unstructured tetrahedral mesh in view of its complicated construction. And the nozzle is discretized with structure hexahedral mesh. The mesh density is designed following the research purpose. The total number of the combination

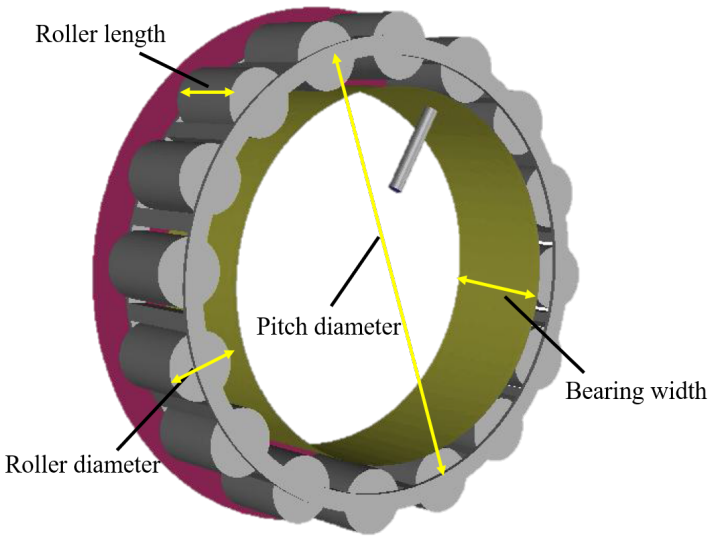

Figure 1: Configuration of the bearing with under-race lubrication

element is about 472,737, with about 108,514 nodes, as shown in Fig. 2. The mesh is built with ANSYS-ICEM.

In the contact regions, the gap between the raceway and rollers is enlarged to avoid mesh distortion. And there is a minimum of 3 elements between the gap at 10 levels of refinement and average y^+ (the dimensionless wall distance) in the range $7 < y^+ < 21$ on the walls. A grid independence test of the numerical solutions has been made primarily, to ensure the validity of numerical results. It's found that a denser mesh changes the calculated results slightly.

The nozzle through the inner race is set as the only velocity inlet of the entire computation domain and the velocity value is determined by different operations. Both end faces of the outlet flow field are specified as the pressure outlet. The reference pressure is the standard atmospheric pressure. Considering the relative rotational motion between the flow field inside the bearing and the flow area of the nozzle, interferences are formed between them to complete data transfer. The standard wall function is adopted for near wall treatment and no-slip boundary condition is adopted at the wall.

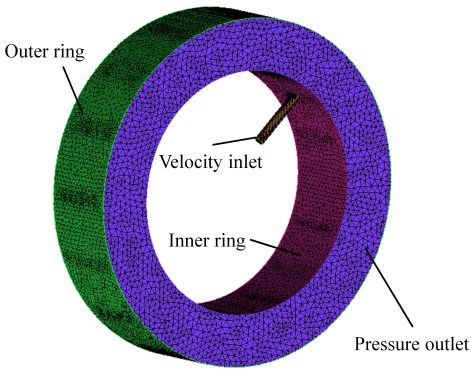

Figure 2: Computational mesh structure and boundary condition

3.2. The CLSVOF two-phase flow model

The analysis of the whole flow passage inside roller bearing with under-race lubrication involves the air and oil two-phase flow. To track the oil/air two-phase flow, the enhanced Coupled Level-Set Volume of Fluid (CLSVOF) method for multiphase flow is used with Reynolds Averaged Navier-Stokes (RANS) equations [23].

In the VOF technique, a colour function, α_{oil}, based on the volume fraction of the oil phase, is used to describe the multiphase mixture of oil and air. In any given cell the following three conditions are possible:

$\alpha_{oil} = 0$ *: The cell is empty of the oil.*

$\alpha_{oil} = 1$ *: The cell is full of the oil.*

$0 < \alpha_{oil} < 1$ *: The cell contains the interface between the oil and air.*

In the Level Set technique, the interface is captured and tracked by a level-set function φ, defined as a signed distance from the interface [24]. Accordingly, the interface is the zero level-set, $\varphi(x,t)$ and can be expressed as $\Gamma =$

$\{x \mid \varphi(x,t) = 0\}$ in a two-phase flow system:

$$\varphi(x,t) = \begin{cases} +|d| & if x \in the primary phase \\ 0 & if x \in \Gamma \\ -|d| & if x \in the secondary phase \end{cases} \tag{1}$$

Where d is the distance from the interface. In the roller bearing, the primary phase means the air and the secondary phase is the injected lubricant oil.

The evolution of the level-set function can be given in a similar fashion as to the VOF model:

$$\frac{\partial \varphi}{\partial t} + \nabla \cdot (\vec{u}\varphi) = 0 \tag{2}$$

where $\vec{u}$ is the underlying velocity field.

And the momentum equation can be written as

$$\frac{\partial (\rho \vec{u})}{\partial t} + \nabla \cdot (\rho \vec{u}\vec{u}) = -\nabla p + \nabla \cdot \mu[\nabla \vec{u} + (\nabla \vec{u})^T] - \vec{F_{sf}} + \rho \vec{g} \tag{3}$$

In the Eq.3, $\vec{F_{sf}}$ is the force arising from surface tension effects given by:

$$\vec{F_{sf}} = \sigma k \delta(\varphi) \vec{n} \tag{4}$$

where: $\sigma = surface tension coefficient$ $k = local mean interface curvature$ $\vec{n} = local interface normal$

and

$$\delta(\varphi) = \begin{cases} 0 & |\varphi| \geq \alpha \\ \frac{1+cos(\pi\varphi/\alpha)}{2\alpha} & |\varphi| < \alpha \end{cases} \tag{5}$$

where $\alpha = 1.5h$ is the thickness of the interface and h is the grid spacing.

In the density correction formulation, Equation 4 is modified by introducing a density ratio:

$$\vec{F_{sf}} = \frac{\rho}{0.5(\rho_1 + \rho_2)} \sigma k \delta(\varphi) \vec{n} \tag{6}$$

where ρ is the volume-based density.

The normal and curvature of the interface, which is needed in the computation of the surface tension force, can be estimated as

$$\vec{n} = \frac{\nabla\varphi}{|\nabla\varphi|} \mid_{\varphi=0} \tag{7}$$

$$k = \nabla \cdot \frac{\nabla\varphi}{|\nabla\varphi|} \mid_{\varphi=0} \tag{8}$$

The coupled Level-Set and VOF approach (CLSVOF) is advised to take advantage of the mass conservation of the VOF method and the sharp interface capturing of the Level-Set method [25]. The values of the VOF and the Level-Set function are both used to reconstruct the interface-front [26]. Namely, the VOF model provides the size of the cut in the cell where the likely interface passes through, and the gradient of the level-set function determines the direction of the interface.

The performance of the CLSVOF method has been evaluated numerically and experimentally, with good agreement [27]. The CLSVOF approach has been proven to have a very good potential and to be suitable for sharp interface simulation inside roller bearings and represent its oil distribution [14].

3.3. Fluid properties

The lubricant oil used here is respected to the MIL-L-23699 type lubricant oil with a popular trade name Mobile Jet 2, and the air is regarded as ideal at atmospheric pressure. Respectively, the lubricant oil density is 976 kg/m^3 while the air density is 1.225 kg/m^3. The viscosity of the oil and air are respectively 0.018 $kg/(m.-s)$ and 1.7894 $\times 10^{-5} kg/(m.-s)$. The surface tension of oil is taken as 0.043 N/m. During the calculations, the oil density is set as constant. With different operating conditions, the oil viscosity is varied to evaluate its effect.

3.4. Numerical Methods

The rotation of inner and outer rings drives rolling elements and the cage. After entering into the bearing, lubricant oil is motivated by orbiting rolling

elements and the cage. The rotating speed of the cage is given as

$$\omega_c = \frac{1}{2}\frac{\omega_i(d_m - d_r)/2 + \omega_o(d_m + d_r)/2}{d_m/2} \tag{9}$$

where ω_m is the rotating speed of the cage, rpm; ω_i and ω_o are the rotating speed of the inner and outer rings respectively, rpm; d_r is the cylinder diameter and d_m is the pitch diameter of the bearing, m.

The CFD codes ANSYS Fluent is proposed to implement the complicated two-phase flow simulations. The finite volume method is used to discretely solve the governing equation. The central difference scheme is adopted for the diffusion and pressure terms of the momentum equation. The second-order upwind difference was adopted for the convection terms. The pressure was adopted for the PRESTO! (PREssure STaggering Option) format. The semi-implicit method for pressure-linked equations-consistent (SIMPLEC) method is adopted for the coupling solution of pressure and velocity.

To model the effect of turbulence in a high-speed rotating condition, the $k-\epsilon$ renormalization group (RNG) turbulence model is employed in this study. The RNG $k-\epsilon$ model considers the influence of high strain rate, large curvature overflowing and other factors, which can improve the accuracy under rotational flow [28].

The explicit CLSVOF formulation with transient time-stepping is used with the Global Courant number kept to less than 0.8 every time step. During the calculations, the convergence of the governing equations is detected by the residuals and the flux conservation of boundaries. The convergence criterion of residual of each velocity component and the volume of fluid function is set to be 10^{-5}, while the convergence criterion of residual of the turbulent kinetic energy and the turbulent kinetic energy dissipation rate is set to be 10^{-4}. In addition, the conservation of mass flow rate of inlet and outlet is monitored. When the net mass flow rate between the inlet and outlet decreases to one percent of the inlet flow rate, the calculation is considered to catch the convergence. The simulation results will be presented in detail.

4. Calculation results

4.1. Nonuniform oil/air distribution

The simulated flow pattern in bearing cavity at different flow time is shown in Fig. 3. The bearing rotates counter-clockwise and the inner ring rotating speed is 5000 rpm. The jet flow rate is about 2.1 L/min, with the nozzle diameter 1.5 mm and the jet velocity 20 m/s. It can been seen that with the calculation time, the oil-phase in bearing cavity increases gradually and occupies the whole circumference. The average oil volume fraction reaches a steady value finally. The nozzle circumferential position changes together with the inner ring's rotating. The oil distribution along the bearing circumference is nonuniform. It gradually increases along the bearing rotating direction and reaches the peak in the position quite close to the nozzle. This phenomenon is similar with that found in jet-cooling ball bearings [13, 14]. Here it is because that most of the lubricant oil flows along the circumferential direction due to the rotating of inner ring and the agitation of the rolling elements and cage. Besides, more oil is thrown to outer ring, not only because of centrifugal force, but also the injecting kinetic energy [29].

The photographs of the flow pattern inside bearing cavity at different rotating speeds (inner ring rotating) are shown in Fig. 4. The inner ring rotating speeds are 5000 rpm, 10000 rpm, 20000 rpm and 40000 rpm, respectively. The injection velocity is 20m/s and the inlet diameter is 1.5mm, with a total oil volume flow rate of 2.1 L/min. It seems that the outer ring race is almost covered with oil phase at 5000 rpm and the bearing is poor-lubricated at 40000 rpm, with most rollers naked in the air phase.

Fig. 5 illustrates oil distribution along the circular of bearing cavity at different inner ring rotating speeds. It could be summarized that, with the increasing of inner ring rotating speed, oil volume fraction in bearing decreases and its distribution along the circumference is getting uniform. The influence of bearing rotating speed will be discussed carefully later.

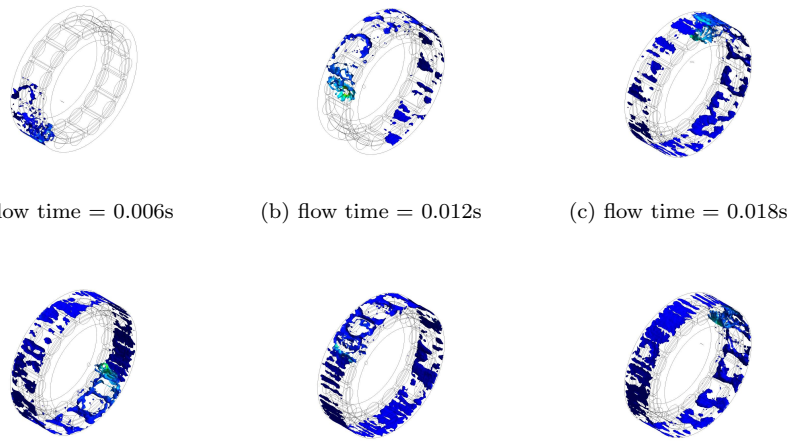

(a) flow time = 0.006s (b) flow time = 0.012s (c) flow time = 0.018s

(d) flow time = 0.024s (e) flow time = 0.030s (f) flow time = 0.036s

Figure 3: Oil distribution evolution inside the bearing cavity with flow time

4.2. Parameters effects to oil volume fraction

It is important to select an appropriate volume fraction of lubricant oil in bearing cavity, since heat generation and bearing temperatures are dependent on this factor [30]. In general, a higher level of oil volume fraction inside bearing cavity has an adverse effect on windage drag and churning losses, while it is beneficial for heat diffusion. So that a balance between these two performance should be catched in the lubrication system design.

Thus, a reasonable estimate of the actual lubricant oil flow rate through bearing cavity must be made, to improve the prediction performance. In this section, different parameters are tested numerically to quantify their effects on the oil volume fraction inside bearing cavity. It is expected primarily that oil volume fraction varies with oil flow rate, rotating speed, nozzle design, and oil property.

4.2.1. The effect of roller rotating by its own axis

In roller bearings, each roller element tranfers along with the cage and rotates by its own axis. It should be noted here that in the numerical investigation,

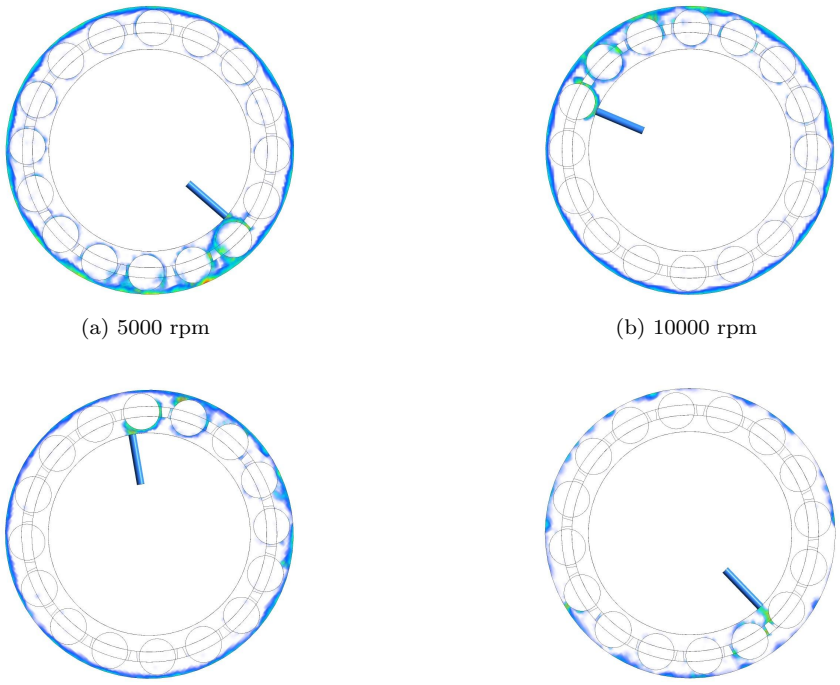

(a) 5000 rpm (b) 10000 rpm

(c) 20000 rpm (d) 40000 rpm

Figure 4: Oil volume fraction contours in the center cross-section with different inner ring rotating speeds

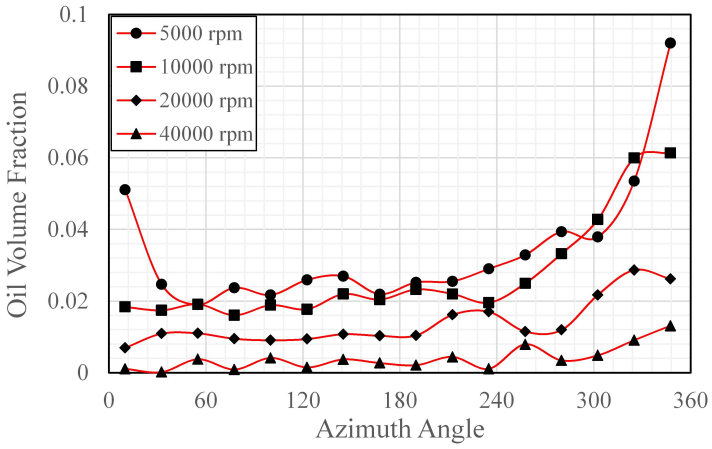

Figure 5: Oil volume fraction distribution around the circumference with different inner ring rotating speeds

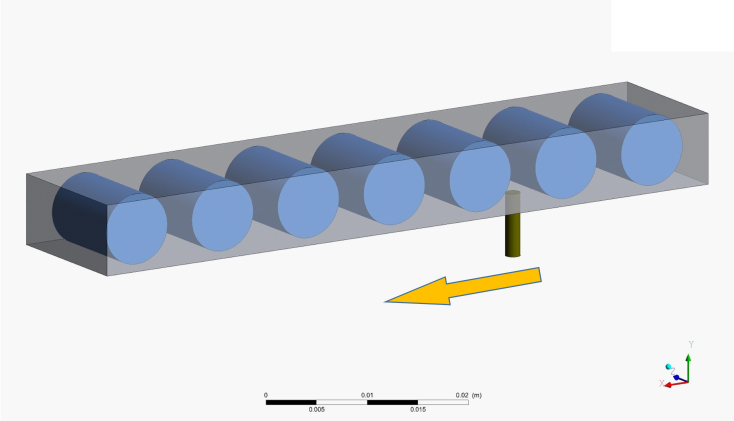

Figure 6: Simulation model for roller rotating validation

the rotating of rollers by its own axis is ignored. Its effect is tested by another configuration, as shown in Fig 6. The oil is injected to a straight box with seven in-line cylinders through a moving nozzle, which represents a simplified approach. The average density of the fluid in the box is monitored during the calculation with different cylinder rotating speeds. The oil property is set as 931 kg/m3, 0.00486 kg/m-s and the nozzle moving speed is 10m/s, with a 20m/s injection velocity. As shown in Fig. 7, it seems that the roller rotating by its own axis slightly changes the average oil volume fraction in the cavity. So that the treatment in the bearing model is acceptable.

4.2.2. Oil volume flow rate

There are two ways to change oil volume flow rate with one single inlet nozzle, to change oil inlet velocity or to change the inlet nozzle diameter. Fig. 8 and Fig. 9 present oil volume fraction as a function of oil volume flow rate or the oil injection velocity with different nozzle diameters. The bearing rotating speed is 5000 rpm. From zero, oil volume fraction increases with the increasing of oil inlet velocity. After reaching the peak value, it decreases with further increasing of oil inlet velocity. This could be explained that, at the first stage, the changing of oil inlet velocity changes oil volume flow rate, which is the dominant element. The oil phase occupies larger region inside the bearing with

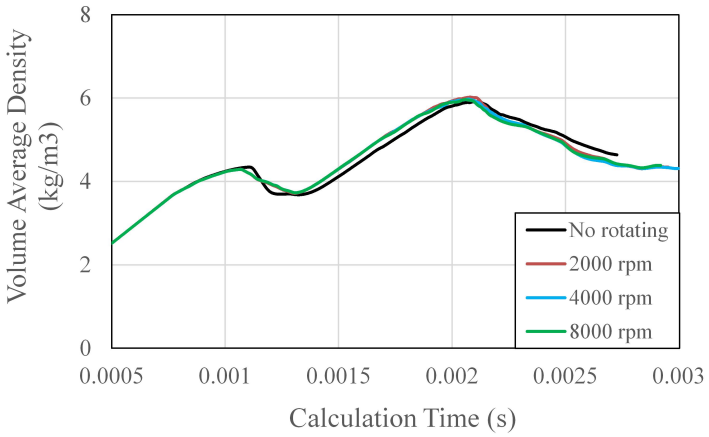

Figure 7: Average fluid density as a function of roller rotating speed

the increasing of oil flow rate. The effect of the impact between injected oil and roller elements is not obvious.

Whereas, after that, the effect of further increasing oil flow rate drops and oil inlet velocity becomes the dominant element, which leads to strong fluid-structure impact. The maximum value of oil volume fraction is reached at oil inlet velocity about 10 m/s for under-race lubrication. At a lower inlet velocity, the oil is hard to enter bearing cavity as a result of the hinder of rolling elements. At a higher inlet velocity, the oil is fired straight to strick with roller elements and flow outside bearing cavity. Hence, the oil inlet velocity needs to be optimised in the design of bearing lubrication system.

With different combination of oil inlet velocity and nozzle diameter, the same oil volume flow rate could be obtained. Fig. 10 shows oil distribution around the circumference with the same oil volume flow rate. The bearing rotating speed is 5000 rpm.

With a higher inlet nozzle diameter, or a lower inlet velocity, a higher oil volume fraction level could be obtained, and the oil distribution is more uniform, as shown in Fig. 11.

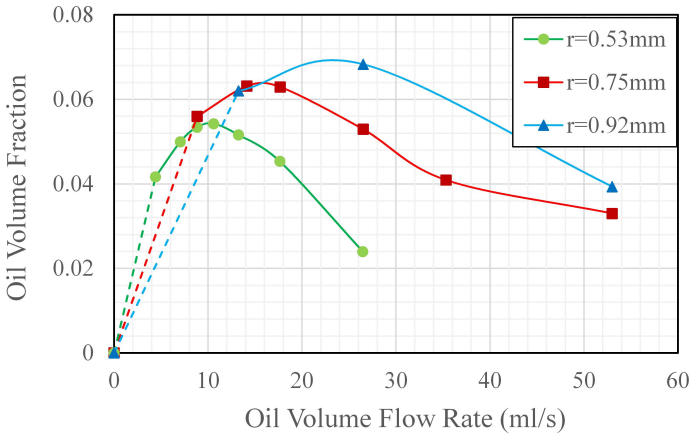

Figure 8: Oil volume fraction as a function of oil volume flow rate

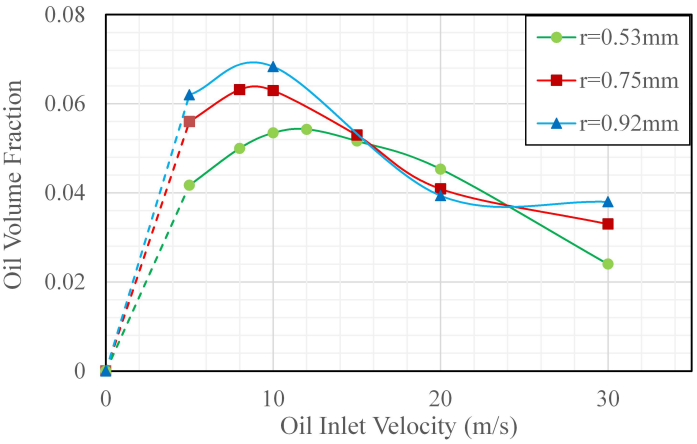

Figure 9: Oil volume fraction as a function of oil inlet vecocity

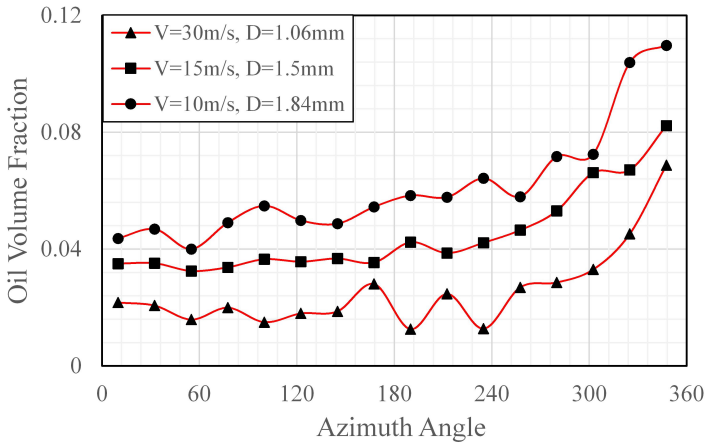

Figure 10: Oil volume fraction distribution with different oil inlet conditions

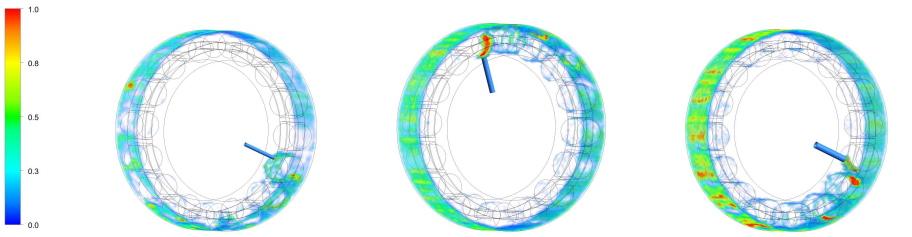

(a) Nozzle diameter = 1.06 mm, Inlet velocity = 30 m/s

(b) Nozzle diameter = 1.5 mm, Inlet velocity = 15 m/s

(c) Nozzle diameter = 1.84 mm, Inlet velocity = 10 m/s

Figure 11: Oil volume fraction contours with different oil inlet conditions

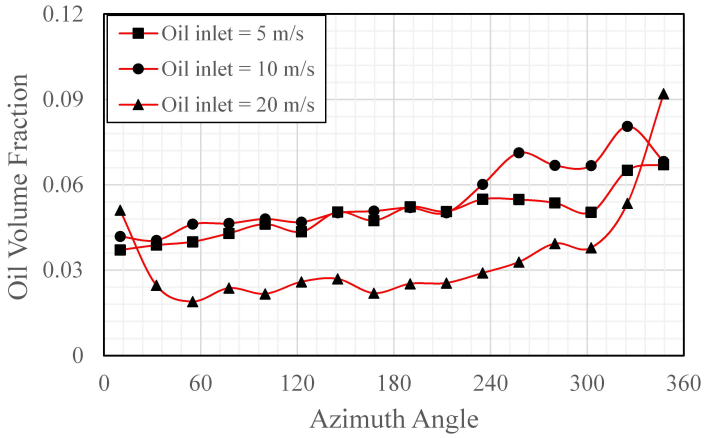

Figure 12: Oil volume fraction distribution with different oil inlet velocity

4.2.3. The oil inlet velocity

Fig. 12 shows oil distribution around the circumference with different oil inlet velocity. The nozzle diameter is fixed to 1.5mm and the bearing rotating speed is 5000 rpm. Fig. 13 shows turbulence kinetic energy distribution in bearing cavity, which demonstrates that the impact between the injected oil and rolling elements is strong with a higher inlet velocity. A higher oil inlet velocity could lead to a higher oil volume flow rate, while at the same time, the impact between the roller and injected oil is heightened. As mentioned above, there is an optimal oil inlet velocity for maximizing oil volume fraction, so that the best way to change oil volume fraction is to change the nozzle diameter or nozzle number.

4.2.4. Oil inlet diameter

For the same oil inlet velocity, a bigger oil inlet diameter leads to a higher oil volume fraction in bearing cavity with the same oil-roller impacting intension, as shown in Fig. 14 and Fig. 15. The oil inlet velocity is 10 m/s and the roller rotating speed is 5000 rpm.

As shown in Fig. 16, the oil volume fraction inside bearing cavity is proportional to oil inlet diameter or oil volume flow rate with the same inlet velocity.

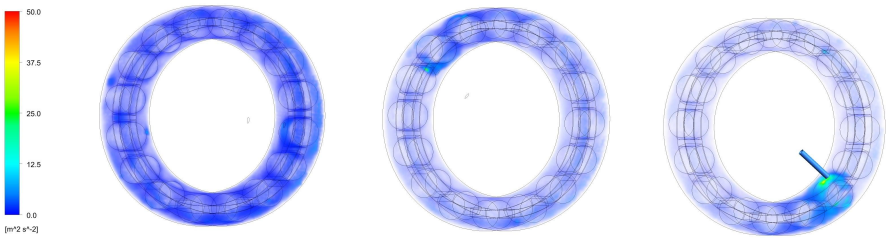

(a) Inlet velocity = 5 m/s (b) Inlet velocity = 10 m/s (c) Inlet velocity = 20 m/s

Figure 13: Turbulence kinetic energy distribution with different oil inlet velocity

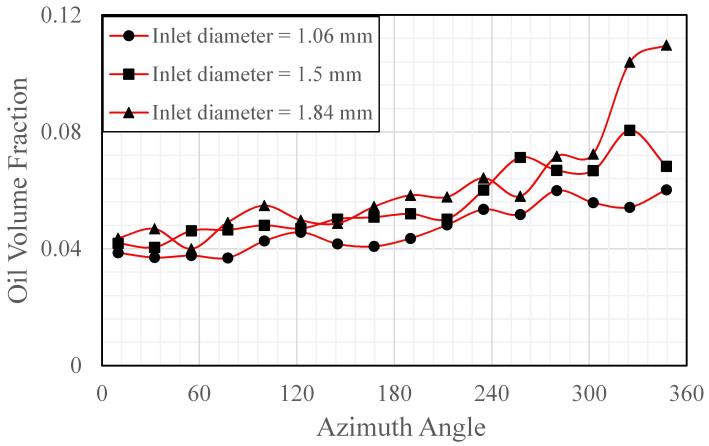

Figure 14: Oil volume fraction distribution with different oil inlet velocity

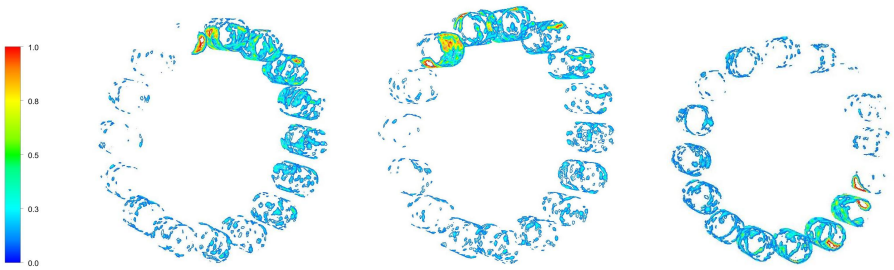

(a) Nozzle diameter = 1.06 mm (b) Nozzle diameter = 1.50 mm (c) Nozzle diameter = 1.84 mm

Figure 15: Oil distribution around the rollers with different nozzle diameters

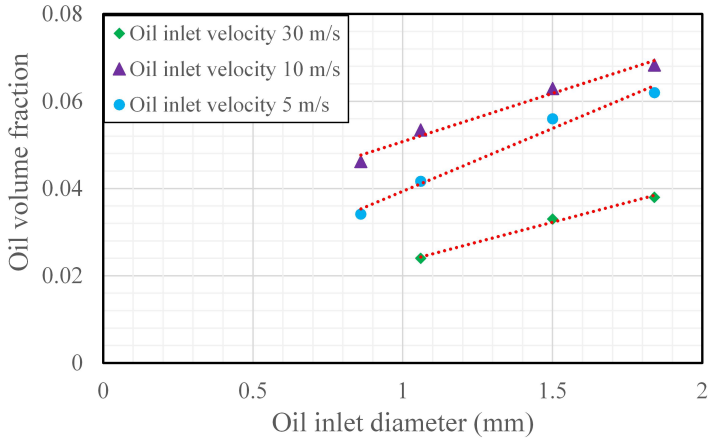

Figure 16: Oil volume fraction as a function of oil inlet diameter

Here it could be found that the oil inlet velocity 10 m/s gets the biggest oil volume fraction, which agrees with that in Fig. 9

4.2.5. Oil viscosity

In Parker' formula [31], all the tests and analysis were performed using MIL-L-23699 type lubricants, so that it could not be used with lubricants whose properties vary significantly from MIL-L-23699.

The fluid viscosity is one of the most important properties for lubricant to determine its lubrication performance. It varies obviously with the lubricant type and its temperature, so that the effect of oil viscosity is studied numerically here.

It is illustrated in Fig. 17 that the air/oil distribution along the circumference is gentler with a higher oil viscosity and the average oil volume fraction inside bearing cavity is about linear to the oil viscosity (as shown in Fig. 18).

4.2.6. Bearing rotating speed

Bearing rotating speed could be regarded as one of the most important parameters that change oil flow in bearing cavity. At the beginning, for the bearing with only inner ring rotating, it has been mentioned that oil volume fraction

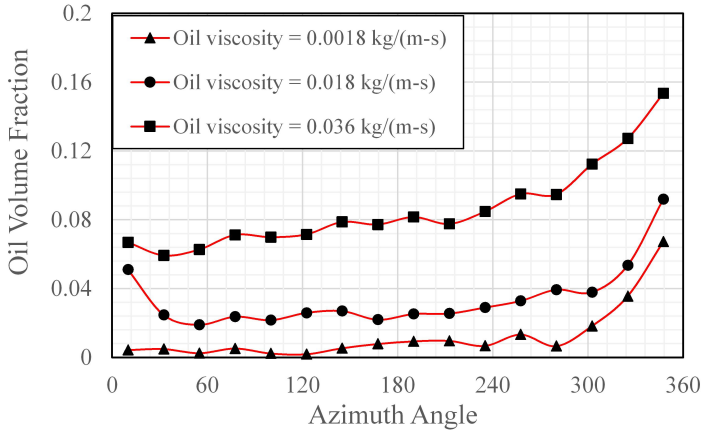

Figure 17: Oil volume fraction distribution with different oil viscosities

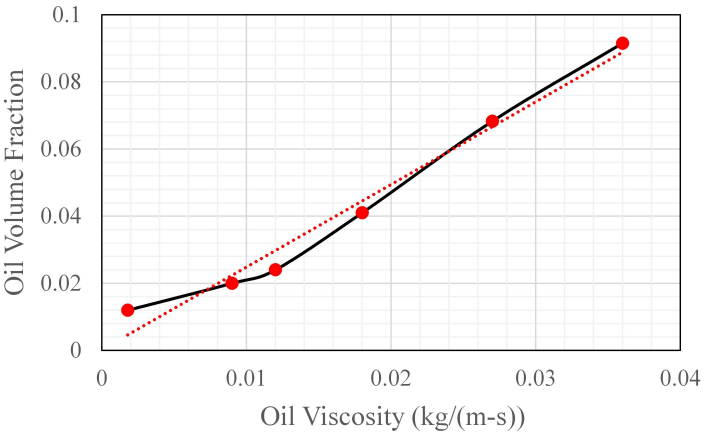

Figure 18: Oil volume fraction as a function of oil viscosity

becomes lower when bearing rotating speed increases. The oil distribution inside the bearing tends to be uniform. But the interaction between the air/oil mixture and bearing components becomes stronger with a higher inner ring rotating speed. In additon, it results in the increase of the fluid flow velocity in the bearing [13].

For the bearing with inner and outer rings rotating together, the rotation of inner ring, the cage, and outer ring, could change oil volume fraction together at the same time. To highlight their individual effect, here these rotational parameters are studied separately. It should be noted that here the relative rotating speed between different components may not follow their relationship in a real bearing.

Inner ring rotating speed

Fig. 19 presents simulated oil volume fraction with different inner ring rotating speed, with the same cage rotating speed (2132 rpm) and fixed outer ring. The oil inlet diameter is 1.5 mm and oil injection velocity is 20 m/s. It can be seen that the oil phase occupies smaller region inside the bearing with higher inner ring rotating speed, which has been verified by Jibin et al. in jet-cooling ball bearings [13]. This can be explained that with a higher inner ring rotating speed, the relative rotating speed between the under-race nozzle and the cage is increased and the interaction between the injected oil and rolling elements becomes stronger. It seems that the average oil volume fraction is linear to the inner ring rotating speed.

Outer ring rotating speed

For inter-shaft supporting roller bearings, outer ring rotates together with inner ring, which may change the air/oil distribution inside bearing cavity.

Fig. 20 illustrates the calculated oil volume fraction with different outer ring rotating speed. In the simulation, the under-race oil nozzle rotates together with inner ring at a speed of 5000 rpm, and the cage rotating speed is fixed to 2132 rpm. The oil inlet diameter is 1.5 mm and oil injection velocity 20 m/s. It could be found that oil volume fraction decreases gradually with the increasing of outer ring rotating speed. Since the rotating speed of inner ring and cage is

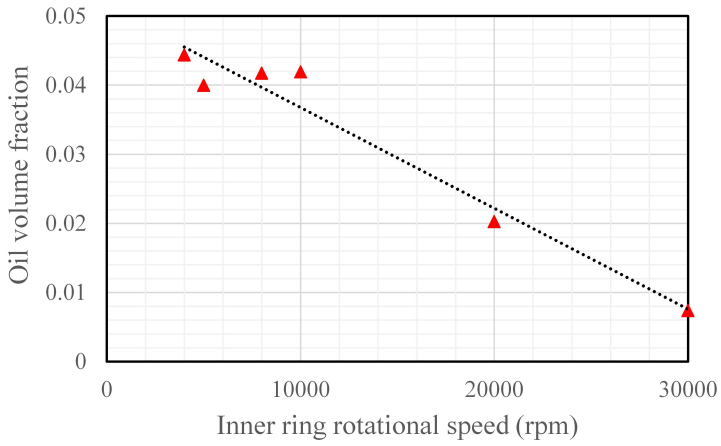

Figure 19: Oil volume fraction as a function of inner ring rotating speed

constant, the changing could only be caused by outer ring rotating. It could contribute to the exhausting of oil phase that gathers on the outer-ring runway, and leads to a linear decrease of oil volume fraction inside bearing cavity.

Cage rotating speed

Except inner and outer rings, the cage rotating may affect oil distribution inside a bearing. Fig. 21 presents the relationship between oil volume fraction and the cage rotating speed. The inner ring rotating speed is fixed to 5000 rpm, with oil inlet diameter 1.5 mm and velocity 20 m/s. We know that the relative rotating speed between inner ring and the cage determines the interaction between the oil and rollers. But here the relative speed decreases at first to zero and then increases with the increasing cage speed. During this process, oil volume fraction decreases continuously. This is because that the oil is forced to flow due to the agitation of rolling elements. With a higher cage rotating speed, oil flow velocity increases and it's easier for the oil to leave bearing cavity. Additionally, the increasing centrifugal force contributes to this behavior, as well.

Inner ring-cage relative rotating speed

Compared with the rotating speed of inner ring or the cage, the effect of the inner ring-cage relative rotating speed is a little confusing. For under-race

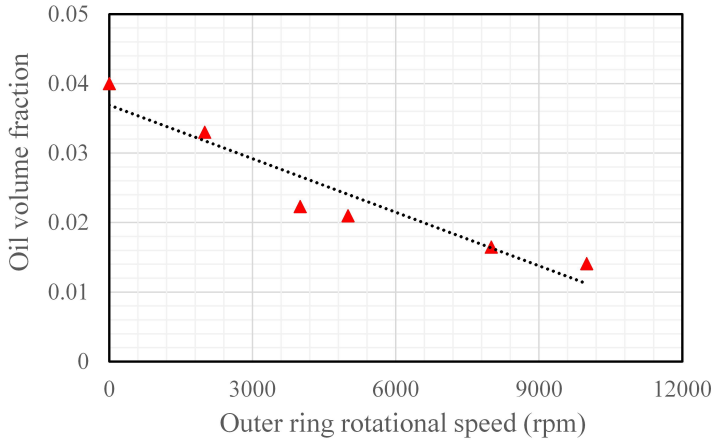

Figure 20: Oil volume fraction distribution as a function of outer ring rotating speed

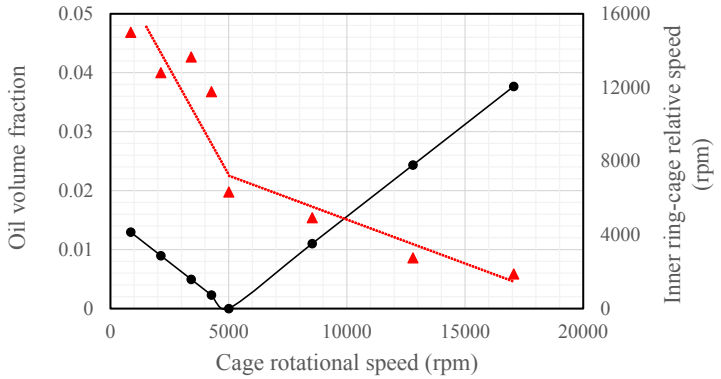

Figure 21: Oil volume fraction as a function of the cage rotating speed

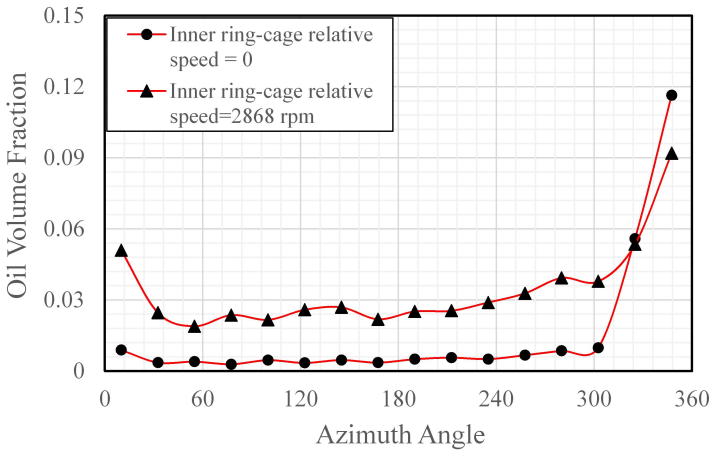

Figure 22: Oil volume fraction distribution with different relative rotating speeds

lubrication, the relative rotating speed is beneficial for sharing the oil phase to the whole circumference of bearing cavity. As shown in Fig. 22, one calculation condition is that the inner and outer rings rotate together at the same rotating speed 5000 rpm so that the cage rotating speed is 5000 rpm and the relative inner ring-cage speed is zero. The other condition is that the inner ring rotates at the speed of 5000 rpm and the cage 2132 rpm. It could be found that without the relative speed, the oil gathers mainly near the region close to the nozzle and the other part of the bearing is poor-lubricated (Fig. 23).

Fig. 24 presents the calculated oil volume fraction inside bearing cavity with different inner ring-cage relative rotating speed. Here the outer ring is fixed. Oil volume fraction increases when the relative rotating speed increases from zero to about 2000 rpm. With the further increase of the relative speed, oil volume fraction decreases. There is a special speed value that can achieve a highest oil distribution. This can be explained that at a small relative speed, the oil is hard to distribute to the whole bearing cavity because of the blocking of rollers near the nozzle. On the other hand, at a very high relative rotating speed, the interaction between the injected oil and rolling elements is strong. The flow velocity of the oil phase is also high, being easier to leave bearing cavity.

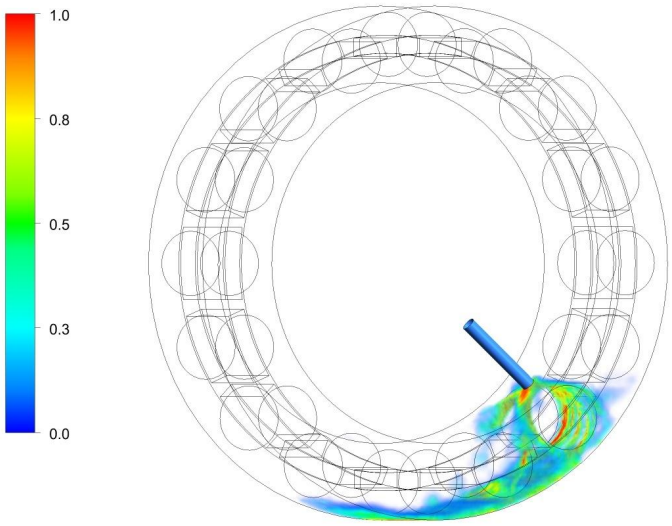

Figure 23: Oil volume fraction distribution with a zero relative rotating speed

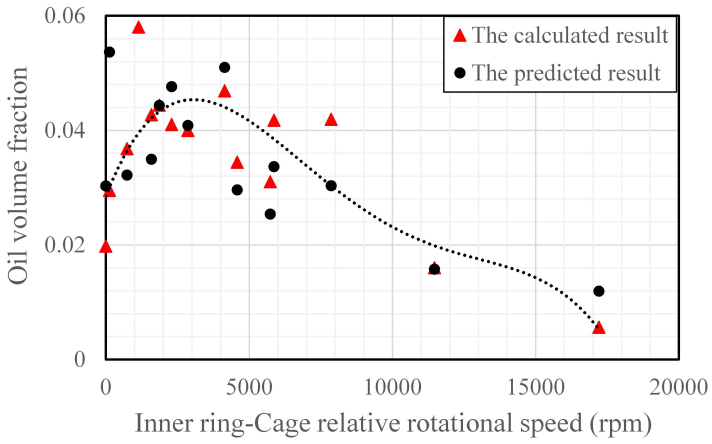

Figure 24: Oil volume fraction as a function of inner ring-cage relative speed

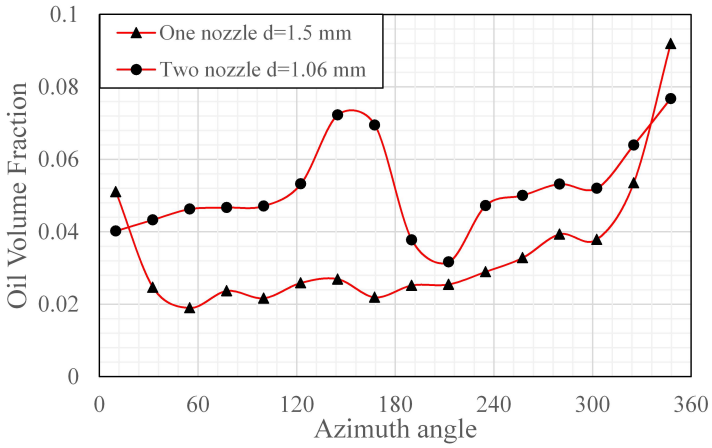

Figure 25: Comparison of oil volume distribution with different inlet nozzle number

4.2.7. Number of nozzles

Fig. 25 compares oil distribution between single-nozzle inlet and dual-nozzle inlets, with the same oil volume flow rate 2.1 L/min and oil inlet velocity 20 m/s. The bearing rotating speed is 5000 rpm. It's found that more oil is kept inside bearing cavity for dual-nozzle inlets. The lowest volume fraction of the oil phase with both single-nozzle inlet and dual-nozzle inlets appears in the upstream side near the nozzle (Fig. 26).

4.2.8. Injection deflection

Fig. 27 illustrates oil volume fraction versus flow time with different inlet nozzle deflection angle. The positive value means the injection direction is natural to the bearing rotating direction (only inner ring rotating), while the negative value means it's inverted. In the numerical simulation, the oil inlet velocity is 20 m/s. The inner ring rotating speed is 5000 rpm and the cage rotating speed is 2132 m/s, with the relative speed of 2868 rpm. The deflection of the inlet nozzle decreases the relative vertical speed between the injected oil and rollers, changing their relative tangential speed. The former has similar effect with changing oil inlet velocity while the latter has the same function as the inner ring-cage relative rotating speed.

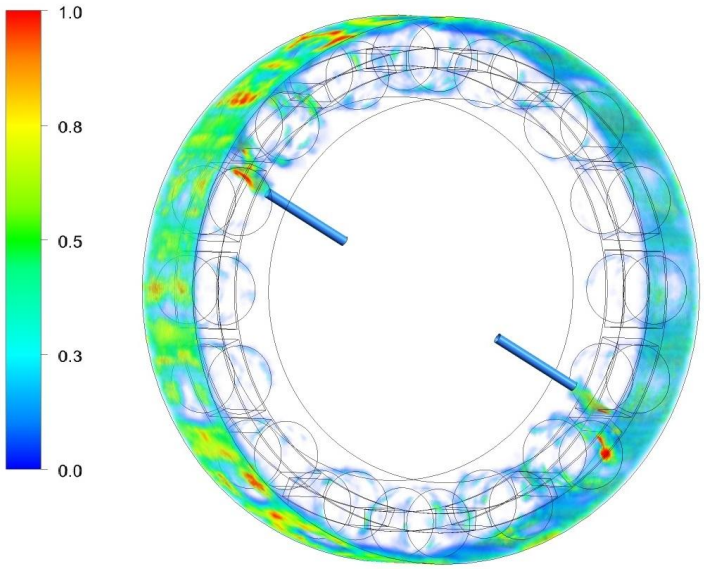

Figure 26: Oil volume fraction distribution with dual-nozzle inlets

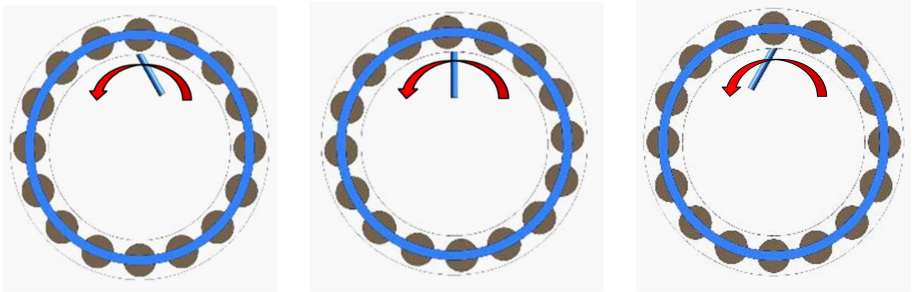

(a) Natural deflection (b) Vertical direction (c) Inverted deflection

Figure 27: Configurations with different oil nozzle deflection directions

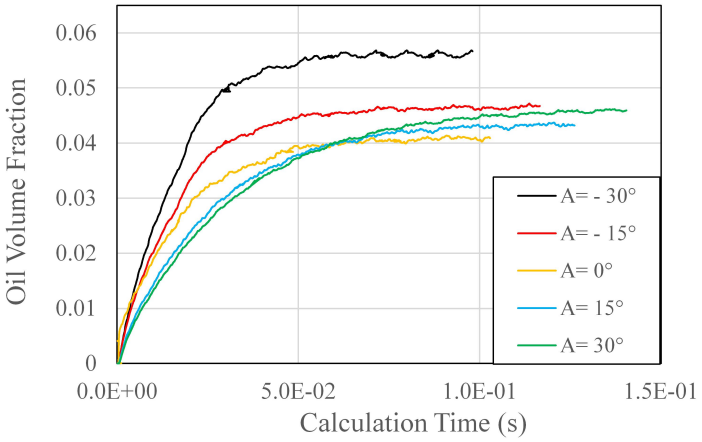

Figure 28: Oil volume fraction distribution with different oil inlet deflection angle

With the conclusion for oil inlet velocity, the decreasing of relative vertical speed could increase the oil volume fraction with the inlet velocity range around 20 m/s, which is corresponding with the results illustrated in Fig. 28. For the natural deflection, the relative tangential speed increases (roller orbiting speed minus tangential component of oil inlet velocity), it is adverse to the increasing of oil volume fraction. While for the reverse deflection, the relative tangential speed is minused, increasing the oil volume fraction. This phenomenon is in agreement with the conclusion about the relative rotating speed in the range bigger than 2000 rpm.

5. Discussion and conclusion

A detailed investigation and effective prediction of the fluid behaviour inside a bearing is essential for appropriate lubricant oil supplying for roller bearings in high speed rotating machinery. In this article, the numerical method is employed to simulate the oil/air two-phase flow inside high speed roller bearings with under-race lubrication. The oil distribution along the circumference between inner and outer rings is studied with different lubricating schemes and operating conditions. Effects of rotating speeds of different bearing components

are investigated in detail.

(1) The oil phase distribution in the bearing is not uniform. It varies with the bearing rotating speed, oil volume flow rate, oil viscosity, etc. There is an optimal oil injection velocity to catch a high level of oil volume fraction inside a bearing.

(2) The average oil volume fraction inside a bearing is proportional to oil viscosity. With a specified oil injection velocity, it is linear to oil inlet diameter.

(3) Rotating speeds of all bearing components could change oil distribution inside a bearing, e.g. inner ring, the cage, and outer ring, including the inner ring-cage relative rotating speed. The results can be used for the precise lubrication design to optimate oil distribution inside a bearing.

Finally, it should be mentioned that the result of the numerical study is sensitive to the simulated geometry and boundary conditions. Now it could only be validated by the form of bearing heat generation prediction [3]. A direct and more reliable experimental validation should be added in the next step, which is our ongoing study.

References

[1] P. Gloeckner, K. Dullenkopf, M. Flouros, Direct outer ring cooling of a high speed jet engine mainshaft ball bearing: experimental investigation results, Journal of Engineering for Gas Turbines and Power 133 (6) (2011) 062503. doi:10.1115/gt2010-23312.

[2] W. Gao, D. Nelias, N. Boisson, Y. Lyu, Model formulation of churning losses in cylindrical roller bearings based on numerical simulation, Tribology International 121 (2018) 420–434. doi:10.1016/j.triboint.2018.02.003.

[3] W. Gao, Y. Lyu, Z. Liu, D. Nelias, Validation and application of a numerical approach for the estimation of drag and churning losses in high speed roller bearings, Applied Thermal Engineering 153 (2019) 390 – 397. doi:https://doi.org/10.1016/j.applthermaleng.2019.03.028.

[4] B. D. Nicholson, G. D. Givan, K. L. Thompson, J. Mason, P. K. Gupta, H. K. Trivedi, Assessment of bearing heat generation prediction by the program adore with respect to experimental results and shaberth predictions, in: ASME Turbo Expo, 2017, p. V001T01A001. doi:10.1115/gt2017-63010.

[5] G. Cavallaro, D. Nelias, F. Bon, Analysis of high-speed intershaft cylindrical roller bearing with flexible rings, Tribology transactions 48 (2) (2005) 154–164. doi:10.1080/05698190590923851.

[6] J. Zhao, Z. Liu, Y. Lu, J. Hu, Numerical modeling of unsteady oil film motion characteristics in bearing chambers, International Journal of Turbo & Jet-Engines 32 (2015) 233–245. doi:10.1515/tjj-2014-0029.

[7] D. Peduto, A. A. Hashmi, K. Dullenkopf, H.-J. Bauer, H. Morvan, Modelling of an aero-engine bearing chamber using enhanced cfd technique, in: ASME 2011 Turbo Expo: Turbine Technical Conference and Exposition, American Society of Mechanical Engineers, 2011, pp. 809–819. doi:10.1115/gt2011-45635.

[8] M. Flouros, C. Salpingidou, K. Yakinthos, M. Hirschmann, F. Cottier, Ejector application for scavenging of an aero engine bearing chamber, Journal of Engineering for Gas Turbines and Power 139 (10) (2017) 101202. doi:10.1115/1.4036516.

[9] A. Bristot, H. P. Morvan, K. A. Simmons, Evaluation of a volume of fluid cfd methodology for the oil film thickness estimation in an aero-engine bearing chamber, in: ASME Turbo Expo 2016, American Society of Mechanical Engineers, 2016, p. V02CT39A007. doi:10.1115/gt2016-56237.

[10] W. Gao, D. Nelias, Y. Lyu, N. Boisson, Numerical investigations on drag coefficient of circular cylinder with two free ends in roller bearings, Tribology International 123 (2018) 43 – 49. doi:https://doi.org/10.1016/j.triboint.2018.02.044.

[11] J. Liebrecht, X. Si, B. Sauer, H. Schwarze, Investigation of drag and churning losses on tapered roller bearings, Journal of Mechanical Engineering 61 (2015) 399–408. doi:10.5545/sv-jme.2015.2490.

[12] W. Wu, C. Hu, J. Hu, S. Yuan, R. Zhang, Jet cooling characteristics for ball bearings using the vof multiphase model, International Journal of Thermal Sciences 116 (2017) 150–158. doi:10.1016/j.ijthermalsci.2017.02.014.

[13] J. Hu, W. Wu, M. Wu, S. Yuan, Numerical investigation of the air–oil two-phase flow inside an oil-jet lubricated ball bearing, International Journal of Heat and Mass Transfer 68 (2014) 85–93. doi:10.1016/j.ijheatmasstransfer.2013.09.013.

[14] W. Wu, J. Hu, S. Yuan, C. Hu, Numerical and experimental investigation of the stratified air-oil flow inside ball bearings, International Journal of Heat and Mass Transfer 103 (2016) 619–626.

[15] W. Wu, C. Hu, J. Hu, S. Yuan, Jet cooling for rolling bearings: Flow visualization and temperature distribution, Applied Thermal Engineering 105 (2016) 217–224. doi:10.1016/j.applthermaleng.2016.05.147.

[16] A. A. Adeniyi, H. Morvan, K. Simmons, A computational fluid dynamics simulation of oil–air flow between the cage and inner race of an aero-engine bearing, Journal of Engineering for Gas Turbines and Power 139 (1) (2017) 012506. doi:10.1115/1.4034210.

[17] K. Yan, Y. Wang, Y. Zhu, J. Hong, Q. Zhai, Investigation on heat dissipation characteristic of ball bearing cage and inside cavity at ultra

high rotation speed, Tribology International 93 (2016) 470–481. doi:10.1016/j.triboint.2015.09.030.

[18] A. A. Adeniyi, H. P. Morvan, K. A. Simmons, A multiphase computational study of oil-air flow within the bearing sector of aeroengines, in: Volume 5C: Heat Transfer, ASME, 2015. doi:10.1115/gt2015-43496.

[19] J. Zhao, Z. Liu, J. Hu, Y. Lyu, Motion of wall oil film with consideration of oil-gas coupled heat and mass transfer in the bearing chamber, Journal of Propulsion Technology 35 (2014) 973–80.

[20] Z. Liu, J. Zhao, J. Hu, Y. Lu, A numerical model for unsteady oil film motion in aero-engine bearing chambers and experimental verification, in: ASME 2013 Gas Turbine India Conference, American Society of Mechanical Engineers, 2013, p. V001T04A007.

[21] J. HU, Z. LIU, Y. LV, J. ZHAO, Comparison of simulation and measurement for film thickness in bearing chamber, Aeronautical Computing Technique 2 (2013) 019.

[22] C. Zhong, J. Hu, Z. Liu, Y. Lu, Y. Hao, Application of the ultrasonic oil film thickness measurement system in bearing chambers, International Journal of Turbo & Jet-Engines 31 (2) (2014) 159–165.

[23] T. Wacławczyk, On a relation between the volume of fluid, level-set and phase field interface models, International Journal of Multiphase Flow 97 (2017) 60–77. doi:10.1016/j.ijmultiphaseflow.2017.08.003.

[24] M. Arienti, M. Sussman, An embedded level set method for sharp-interface multiphase simulations of diesel injectors, International Journal of Multiphase Flow 59 (2014) 1–14. doi:10.1016/j.ijmultiphaseflow.2013.10.005.

[25] Z. Shang, J. Lou, H. Li, Simulations of flow transitions in a vertical pipe using coupled level set and VOF method, International Jour-

nal of Computational Methods 14 (02) (2017) 1750013. doi:10.1142/s021987621750013x.

[26] J. Xu, Y. Huang, M. Lai, Z. Li, A coupled immersed interface and level set method for three-dimensional interfacial flows with insoluble surfactant, Communications in Computational Physics 15 (2) (2014) 451–469. doi:10.4208/cicp.241012.310513a.

[27] Y. Guo, L. Wei, G. Liang, S. Shen, Simulation of droplet impact on liquid film with CLSVOF, International Communications in Heat and Mass Transfer 53 (2014) 26–33. doi:10.1016/j.icheatmasstransfer.2014.02.006.

[28] J. Xiao, E. Zhu, G. Wang, Numerical simulation of emergency shutdown process of ring gate in hydraulic turbine runaway, Journal of Fluids Engineering 134 (12) (2012) 124501. doi:10.1115/1.4007971.

[29] K. Yan, J. Zhang, J. Hong, Y. Wang, Y. Zhu, Structural optimization of lubrication device for high speed angular contact ball bearing based on internal fluid flow analysis, International Journal of Heat and Mass Transfer 95 (2016) 540–550. doi:10.1016/j.ijheatmasstransfer.2015.12.036.

[30] K. Yan, Y. Wang, Y. Zhu, J. Hong, Investigation on the effect of sealing condition on the internal flow pattern of high-speed ball bearing, Tribology International 105 (2017) 85–93. doi:10.1016/j.triboint.2016.09.032.

[31] R. J. Parker, Comparison of predicted and experimental thermal performance of angular-contact ball bearings.